Electrons on the honeycomb lattice

Subir Sachdev
Department of Physics, Harvard University,
Cambridge, Massachusetts, 02138, USA

(Dated: February 26, 2018)

Abstract

Notes adapted from

Quantum Phase Transitions by S. Sachdev, Cambridge University Press, and

String Theory and Its Applications, TASI 2010, From meV to the Planck Scale, Proceedings of the 2010 Theoretical Advanced Study Institute in Elementary Particle Physics, Boulder, Colorado, 1-25 June 2010, World Scientific (2011), arXiv:1012.0299.

CONTENTS

I. ELECTRON HUBBARD MODEL ON THE HONEYCOMB LATTICE

The electron Hubbard model is defined by the Hamiltonian

$$H = -\sum_{i,j} t_{ij} c^\dagger_{i\alpha} c_{j\alpha} + \sum_i \left[-\mu \left(n_{i\uparrow} + n_{i\downarrow} \right) + U_i \left(n_{i\uparrow} - \frac{1}{2} \right) \left(n_{i\downarrow} - \frac{1}{2} \right) \right]. \tag{1}$$

Here $c_{i\alpha}$, $\alpha = \uparrow, \downarrow$ are annihilation operators on the site i of a regular lattice, and t_{ij} is a Hermitian, short-range matrix containing the 'hopping matrix elements' which move the electrons between different lattice sites. The density of electrons is controlled by the chemical potential μ which couples to the total electron density, with

$$n_{i\uparrow} \equiv c^\dagger_{i\uparrow} c_{i\uparrow} \quad , \quad n_{i\downarrow} \equiv c^\dagger_{i\downarrow} c_{i\downarrow}. \tag{2}$$

The electrons repel each other with an on-site interaction U_i; in most cases we will take $U_i = U$ site-independent, but it will also be useful later to allow for a site-dependent U_i. For completeness, we also note the algebra of the fermion operators:

$$\begin{aligned} c_{i\alpha} c^\dagger_{j\beta} + c^\dagger_{j\beta} c_{i\alpha} &= \delta_{ij} \delta_{\alpha\beta} \\ c_{i\alpha} c_{j\beta} + c_{j\beta} c_{i\alpha} &= 0. \end{aligned} \tag{3}$$

The equations (1), (2), and (3) constitute a self-contained and complete mathematical statement of the problem of the landscape of the Hubbard model. It is remarkable that a problem that is so simple to state has such a rich phase structure as a function of the lattice choice, the fermion density, and the spatial forms of t_{ij} and U_i.

A. Preliminaries

We will consider the Hubbard model (1) with the sites i on locations $\boldsymbol{r}_i$ on the honeycomb lattice shown in Fig. 1 at a density of one electron per site ("half-filling"), so that $\langle n_{i\uparrow} \rangle = \langle n_{i\downarrow} \rangle = 1/2$. Here, we set up some notation allowing us to analyze the geometry of this lattice.

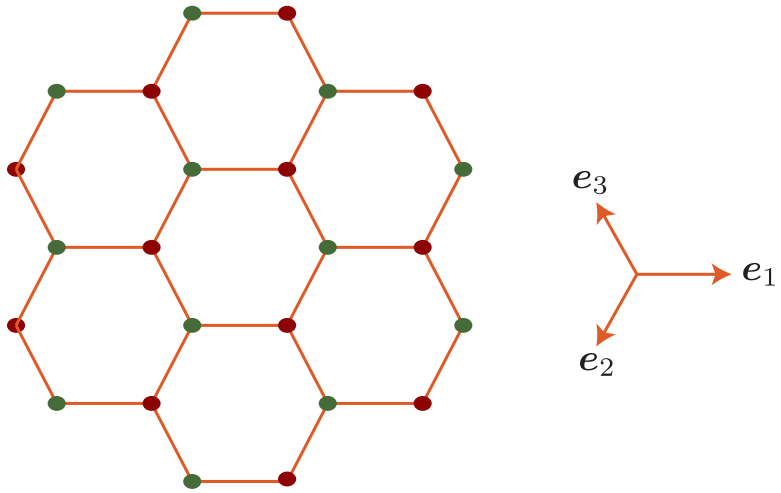

FIG. 1. The honeycomb lattice with its A (green) and B (red) sublattices

We work with a lattice with unit nearest neighbor spacing. We define unit length vectors which connect nearest-neighbor sites

$$\boldsymbol{e}_1 = (1,0) \quad , \quad \boldsymbol{e}_2 = (-1/2, \sqrt{3}/2) \quad , \quad \boldsymbol{e}_3 = (-1/2, -\sqrt{3}/2). \tag{4}$$

Note that $\boldsymbol{e}_i \cdot \boldsymbol{e}_j = -1/2$ for $i \neq j$, and $\boldsymbol{e}_1 + \boldsymbol{e}_2 + \boldsymbol{e}_3 = 0$. The lattice can be divided into the A and B sublattices, as shown in Fig. 1. We take the origin of co-ordinates of the lattice at the center of an *empty hexagon*. The A sublattice sites closest to the origin are at $\boldsymbol{e}_1$, $\boldsymbol{e}_2$, and $\boldsymbol{e}_3$, while the B sublattice sites closest to the origin are at $-\boldsymbol{e}_1$, $-\boldsymbol{e}_2$, and $-\boldsymbol{e}_3$.

The unit cell of the hexagonal lattice contains 2 sites, one each from the A and B sublattices. These unit cells form a triangular Bravais lattice consisting of the centers of the hexagons. The triangular lattice points closest to the origin are $\pm(\boldsymbol{e}_1 - \boldsymbol{e}_2)$, $\pm(\boldsymbol{e}_2 - \boldsymbol{e}_3)$, and $\pm(\boldsymbol{e}_3 - \boldsymbol{e}_1)$. The reciprocal lattice is a set of wavevectors $\boldsymbol{G}$ such that $\boldsymbol{G} \cdot \boldsymbol{r} = 2\pi \times$ integer, where $\boldsymbol{r}$ is the center of any hexagon of the honeycomb lattice. The reciprocal lattice is also a triangular lattice, and it consists of the points $\sum_i n_i \boldsymbol{G}_i$, where n_i are integers and

$$\boldsymbol{G}_1 = \frac{4\pi}{3}\boldsymbol{e}_1 \quad , \quad \boldsymbol{G}_2 = \frac{4\pi}{3}\boldsymbol{e}_2 \quad , \quad \boldsymbol{G}_3 = \frac{4\pi}{3}\boldsymbol{e}_3. \tag{5}$$

The unit cell of the reciprocal lattice is called the first Brillouin zone. This is a hexagon whose vertices are given by

$$\boldsymbol{Q}_1 = \frac{1}{3}(\boldsymbol{G}_2 - \boldsymbol{G}_3) \quad , \quad \boldsymbol{Q}_2 = \frac{1}{3}(\boldsymbol{G}_3 - \boldsymbol{G}_1) \quad , \quad \boldsymbol{Q}_3 = \frac{1}{3}(\boldsymbol{G}_1 - \boldsymbol{G}_2), \tag{6}$$

and $-\boldsymbol{Q}_1$, $-\boldsymbol{Q}_2$, and $-\boldsymbol{Q}_3$; see Fig. 2. Integrals and sums over momentum space will implicitly extend only over the first Brillouin zone. This is the 'ultraviolet cutoff' imposed by the underlying lattice structure.

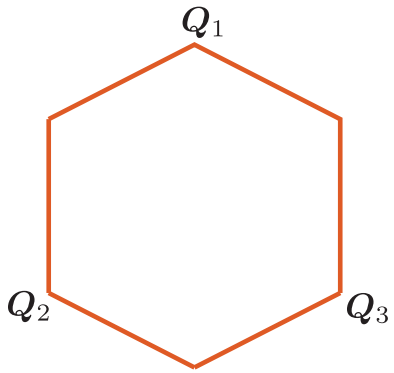

FIG. 2. The first Brillouin zone of the honeycomb lattice.

We define the Fourier transform of the electrons on the A sublattice by

$$c_{A\alpha}(\boldsymbol{k}) = \frac{1}{\sqrt{\mathcal{N}}} \sum_{i \in A} c_{i\alpha} e^{-i\boldsymbol{k}\cdot\boldsymbol{r}_i}, \tag{7}$$

where $\mathcal{N}$ is the number of sites on one sublattice; similarly for $c_{B\alpha}$. Note that $c_{A\alpha}(\boldsymbol{k}+\boldsymbol{G}) = c_{A\alpha}(\boldsymbol{k})$: consequently, sums over momentum have to be restricted to the first Brillouin zone to avoid double counting. Thus the inverse of Eq. (7) sums over $\boldsymbol{k}$ in the first Brillouin zone.

B. Semi-metal

We begin with free electrons in the honeycomb lattice, $U = 0$, with only nearest-neighbor electron hopping $t_{ij} = t$. Using Eq. (7), we can write the hopping Hamiltonian as

$$\begin{aligned} H_0 = &-t \sum_{\boldsymbol{k}} \left(e^{i\boldsymbol{k}\cdot\boldsymbol{e}_1} + e^{i\boldsymbol{k}\cdot\boldsymbol{e}_2} + e^{i\boldsymbol{k}\cdot\boldsymbol{e}_3} \right) c^\dagger_{A\alpha}(\boldsymbol{k}) c_{B\alpha}(\boldsymbol{k}) + \text{H.c.} \\ &-\mu \sum_{\boldsymbol{k}} \left(c^\dagger_{A\alpha}(\boldsymbol{k}) c_{A\alpha}(\boldsymbol{k}) + c^\dagger_{B\alpha}(\boldsymbol{k}) c_{B\alpha}(\boldsymbol{k}) \right) \end{aligned} \tag{8}$$

We introduce Pauli matrices τ^a $(a = x, y, z)$ which act on the A, B sublattice space; then this Hamiltonian can be written as

$$\begin{aligned} H_0 = \sum_{\boldsymbol{k}} c^\dagger(\boldsymbol{k}) \Big[&-\mu - t\Big(\cos(\boldsymbol{k}\cdot\boldsymbol{e}_1) + \cos(\boldsymbol{k}\cdot\boldsymbol{e}_2) + \cos(\boldsymbol{k}\cdot\boldsymbol{e}_3)\Big)\tau^x \\ &+ t\Big(\sin(\boldsymbol{k}\cdot\boldsymbol{e}_1) + \sin(\boldsymbol{k}\cdot\boldsymbol{e}_2) + \sin(\boldsymbol{k}\cdot\boldsymbol{e}_3)\Big)\tau^y \Big] c(\boldsymbol{k}), \end{aligned} \tag{9}$$

where the sublattice and spin indices on the electrons are now implicit: the $c(\boldsymbol{k})$ are 4-component fermion operators.

The energy eigenvalues are easily determined to be

$$-\mu \pm \left| e^{i\boldsymbol{k}\cdot\boldsymbol{e}_1} + e^{i\boldsymbol{k}\cdot\boldsymbol{e}_2} + e^{i\boldsymbol{k}\cdot\boldsymbol{e}_3} \right| \tag{10}$$

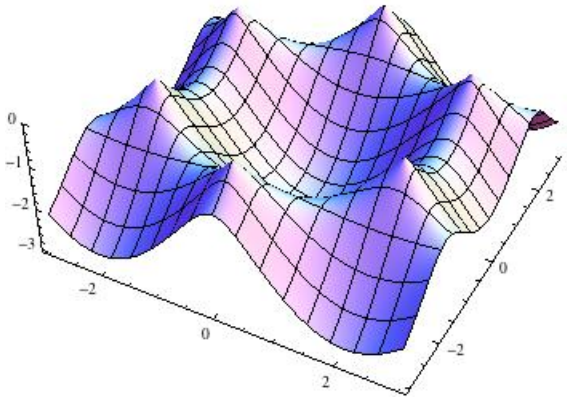

FIG. 3. The lower band of the dispersion in Eq. (10) for $\mu = 0$

and these are plotted in Fig. 3. At half-filling, exactly half the states should be occupied in the ground state, and for the spectrum in Eq. (10) this is achieved at $\mu = 0$.

A crucial feature of any metallic state is the Fermi surface: this is boundary between the occupied and empty states in momentum space. In two spatial dimensions, this boundary is generically a line in momentum space, and this is the case for the dispersion in Eq. (10) for $\mu \neq 0$. However, for the $\mu = 0$, the honeycomb lattice has the special property that the occupied and empty states meet only at a discrete set of single points in momentum space: this should be clear from the dispersion plotted in Fig. 3. Only 2 of these points are distinct, in that they are not separated by a reciprocal lattice vector $\boldsymbol{G}$. So the half-filled honeycomb lattice has 2 'Fermi points', and realizes a 'semi-metal' phase. The low energy excitations of the semi-metal consist of particles and holes across the Fermi point, and these have a lower density of states than in a metallic phase with a Fermi line. We also note that the Fermi-point structure is protected by a sublattice exchange symmetry: it is not special to the nearest-neighbor hopping model, and it also survives the inclusion of electron-electron interactions.

We obtain a very useful, and universal, theory for the low energy excitations of the semi-metal by expanding (9) in the vicinity of the Fermi points. The distinct Fermi points are present at $\boldsymbol{Q}_1$ and $-\boldsymbol{Q}_1$; all other Fermi points are separated from these two points by a reciprocal lattice vector $\boldsymbol{G}$. So we define continuum Fermi field which reside in 'valleys' in the vicinity of these points by

$$\begin{aligned} C_{A1\alpha}(\boldsymbol{k}) &= \sqrt{A}\, c_{A\alpha}(\boldsymbol{Q}_1 + \boldsymbol{k}) \\ C_{A2\alpha}(\boldsymbol{k}) &= \sqrt{A}\, c_{A\alpha}(-\boldsymbol{Q}_1 + \boldsymbol{k}) \\ C_{B1\alpha}(\boldsymbol{k}) &= \sqrt{A}\, c_{B\alpha}(\boldsymbol{Q}_1 + \boldsymbol{k}) \\ C_{B2\alpha}(\boldsymbol{k}) &= \sqrt{A}\, c_{B\alpha}(-\boldsymbol{Q}_1 + \boldsymbol{k}), \end{aligned} \tag{11}$$

where A is the total area of the honeycomb lattice, and the momentum $\boldsymbol{k}$ is small. The field

C is a 8-component continuum canonical Fermi field: the components correspond to spin ($\uparrow$, $\downarrow$), sublattice (A, B), and valley $(1, 2)$ indices. We will also use Pauli matrices which act on the spin (σ^a), sublattice (τ^a), and valley (ρ^a) space.

Inserting Eq. (11) into Eq. (9), we obtain the continuum Hamiltonian

$$H_0 = \int \frac{d^2k}{4\pi^2} C^\dagger(\boldsymbol{k}) \Big(v\tau^y k_x + v\tau^x \rho^z k_y \Big) C(\boldsymbol{k}), \tag{12}$$

where $v = 3t/2$. From now on we rescale time to set $v = 1$. Diagonalizing Eq. (12), we obtain the relativistic spectrum

$$\pm \sqrt{k_x^2 + k_y^2}, \tag{13}$$

which corresponds to the values of Eq. (10) near the Fermi points.

The relativistic structure of H_0 can be made explicit by rewriting it as the Lagrangian of massless Dirac fermions. Define $\overline{C} = C^\dagger \rho^z \tau^z$. Then we can write the Euclidean time (τ) Lagrangian density of the semi-metal phase as

$$\mathcal{L}_0 = \overline{C} \left(\partial_\tau \gamma_0 + \partial_x \gamma_1 + \partial_y \gamma_2 \right) C \tag{14}$$

where ω is the frequency associated with imaginary time, and the Dirac γ matrices are

$$\gamma_0 = -\rho^z \tau^z \quad \gamma_1 = \rho^z \tau^x \quad \gamma_2 = -\tau^y. \tag{15}$$

In addition to relativistic invariance, this form makes it clear the free-fermion Lagrangian has a large group of 'flavor' symmetries that acts on the 8×8 fermion space and commute with the γ matrices. Most of these symmetries are not obeyed by higher-order gradients, or by fermion interaction terms which descend from the Hubbard model.

Let us now turn on a small repulsion, U, between the fermions in the semi-metal. Because of the point-like nature of the Fermi surface, it is easier to determine the consequences of this interaction here than in a metallic phase with a Fermi line of gapless excitations. We can use traditional renormalization group (RG) methods to conclude that a weak U is irrelevant in the infrared. Consequently, the semi-metal state is a stable phase which is present over a finite range of parameters.

C. Antiferromagnet

Although a small U is irrelevant, new phases can and do appear at large U. To see this, let us return to the lattice Hubbard model in Eq. (1), and consider the limit of large $U_i = U$. We will assume $\mu = 0$ and half-filling in the remainder of this section.

At $U = \infty$, the eigenstates are simple products over the states on each site. Each site has 4 states:

$$|0\rangle \quad , \quad c_{i\uparrow}^\dagger |0\rangle \quad , \quad c_{i\downarrow}^\dagger |0\rangle \quad , \quad c_{i\uparrow}^\dagger c_{i\downarrow}^\dagger |0\rangle, \tag{16}$$

where $|0\rangle$ is the empty state. The energies of these states are $U/4$, $-U/4$, $-U/4$, and $U/4$ respectively. Thus the ground state on each site is doubly-degenerate, corresponding to the spin-up and spin-down states of a single electron. The lattice model has a degeneracy of $2^{2\mathcal{N}}$, and so a non-zero entropy density (recall that $\mathcal{N}$ is the number of sites on one sublattice).

Any small perturbation away from the $U = \infty$ limit is likely to lift this exponential large degeneracy. So we need to account for the electron hopping t. At first order, electron hopping moves an electron from one singly-occupied site to another, yielding a final state with one empty and one doubly occupied site. This final state has an energy U higher than the initial state, and so is not part of the low energy manifold. So by the rules of degenerate perturbation theory, there is no correction to the energy of all the $2^{2\mathcal{N}}$ ground states at first order in t.

At second order in t, we have to use the effective Hamiltonian method. This performs a canonical transformation to eliminate the couplings from the ground states to all the states excited by energy U, while obtaining a modified Hamiltonian which acts on the $2^{2\mathcal{N}}$ ground states. This method is described in text books on quantum mechanics. The resulting effective Hamiltonian is the Heisenberg antiferromagnet:

$$H_J = \sum_{i<j} J_{ij} S_i^a S_j^a \quad , \quad J_{ij} = \frac{4t_{ij}^2}{U}, \tag{17}$$

where J_{ij} is the exchange interaction and S_i^a are the spin operators on site i

$$S_i^a = \frac{1}{2} c_{i\alpha}^\dagger \sigma_{\alpha\beta}^a c_{i\beta}. \tag{18}$$

Note that these spin operators preserve the electron occupation number on every site, and so act within the subspace of the $2^{2\mathcal{N}}$ low energy states. The Hamiltonian H_J lifts the macroscopic degeneracy, and the entropy density of the new ground state will be zero.

Although we cannot compute the exact ground state of H_J on the honeycomb lattice with nearest-neighbor exchange, numerical studies [1] leave little doubt to its basic structure. The ground state is adiabatically connected to that obtained by treating the S_i^a as classical vectors in spin space: it has antiferromagnetic (or Néel) order which breaks the global SU(2) spin rotation symmetry, by a spontaneous polarization of the spins on opposite orientations on the two sublattices

$$\eta_i \langle S_i^a \rangle = N^a, \tag{19}$$

where $\eta_i = 1$ ($\eta_i = -1$) on sublattice A (B), and N^a is the vector Néel order parameter; see Fig. 4. Classically this state minimizes the exchange coupling in Eq. (17) because $J_{ij} > 0$. Quantum fluctuations for spin $S = 1/2$ reduce the spontaneous moment from its classical value, but a non-zero moment remains on the honeycomb lattice.

What is the electronic excitation spectrum in the antiferromagnet? To determine this, it is useful to write the Néel order parameter in terms of the continuum Dirac fields introduced in

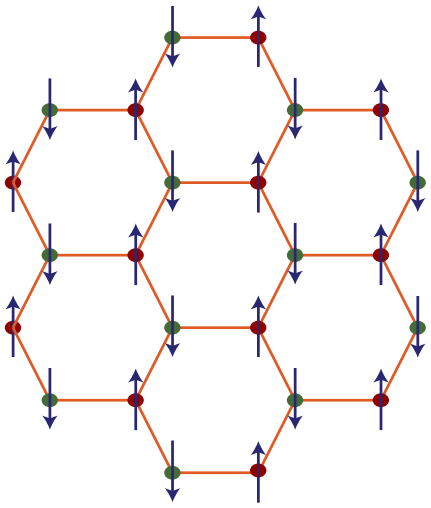

FIG. 4. The large U state with antiferromagnetic (Néel) order.

Section I B. We observe

$$\sum_i \eta_i S_i^a = \sum_{\boldsymbol{k}} \left(c^\dagger_{A\alpha} \sigma^a_{\alpha\beta} c_{A\beta} - c^\dagger_{B\alpha} \sigma^a_{\alpha\beta} c_{B\beta} \right) = \int \frac{d^2k}{4\pi^2} C^\dagger \tau^z \sigma^a C \tag{20}$$

Thus the Néel order parameter N^a is given by the fermion bilinear

$$N^a = \left\langle C^\dagger \tau^z \sigma^a C \right\rangle = \left\langle \overline{C} \rho^z \sigma^a C \right\rangle, \tag{21}$$

and the vacuum expectation value (VEV) is non-zero in the antiferromagnet. We can expect that electron-electron interactions will induce a coupling between the fermion excitations and this VEV in the low energy Hamiltonian for the Néel phase. Choosing Néel ordering in the z direction

$$N^a = N_0 \delta_{az}, \tag{22}$$

we anticipate that H_0 in Eq. (12) is modified in the Néel phase to

$$H_N = \int \frac{d^2k}{4\pi^2} C^\dagger(\boldsymbol{k}) \left(\tau^y k_x + \tau^x \rho^z k_y - \lambda N_0 \tau^z \sigma^z \right) C(\boldsymbol{k}), \tag{23}$$

where λ is a coupling determined by the electron interactions, and we have assumed Néel order polarized in the z direction. This effective Hamiltonian will be explicitly derived in the next subsection. We can now easily diagonalize H_N to deduce that the electronic excitations have energy

$$\pm \sqrt{k_x^2 + k_y^2 + \lambda^2 N_0^2}. \tag{24}$$

This is the spectrum of massive Dirac fermions. So the Fermi point has disappeared, and an energy gap has opened in the fermion excitation spectrum. In condensed matter language, the phase with antiferromagnetic order is an insulator, and not a semi-metal: transmission of electronic charge will require creation of gapped particle and hole excitations.

D. Quantum phase transition

We have now described a semi-metal phase for small U, and an antiferromagnetic insulator for large U. Both are robust phases, whose existence has been reliably established. We now consider connecting these two phases at intermediate values of U [1].

We can derive the field theory for this direct transition either by symmetry considerations, or by an explicit derivation from the Hubbard model. Let us initially follow the second route. We start with the Hubbard Hamiltonian in Eq. (1), use the operator identity (valid on each site i):

$$U\left(n_\uparrow - \frac{1}{2}\right)\left(n_\downarrow - \frac{1}{2}\right) = -\frac{2U}{3}S^{a2} + \frac{U}{4}. \tag{25}$$

Then, in the fermion coherent state path integral for the Hubbard model, we apply a 'Hubbard-Stratonovich' transformation to the interaction term; this amounts to using the identity

$$\begin{aligned}&\exp\left(\frac{2U}{3}\sum_i \int d\tau S_i^{a2}\right)\\ &= \int \mathcal{D}X_i^a(\tau)\exp\left(-\sum_i \int d\tau\left[\frac{3}{8}X_i^{a2} - \sqrt{U}X_i^a S_i^a\right]\right)\end{aligned} \tag{26}$$

The fermion path integral is now a bilinear in the fermions, and we can, at least formally, integrate out the fermions in the form of a functional determinant. We imagine doing this temporarily, and then look for the saddle point of the resulting effective action for the X_i^a. At the saddle-point we find that the lowest energy is achieved when the vector has opposite orientations on the A and B sublattices. Anticipating this, we look for a continuum limit in terms of a field φ^a where

$$X_i^a = \eta_i \varphi^a \tag{27}$$

Using Eq. (20), the continuum limit of the coupling between the field φ^a and the fermions in Eq. (26) is given by

$$X_i^a c_{i\alpha}^\dagger \sigma^a_{\alpha\beta} c_{i\beta} = \varphi^a C^\dagger \tau^z \sigma^a C = \varphi^a \overline{C}\rho^z \sigma^a C \tag{28}$$

From this it is clear that φ^a is a dynamical quantum field which represents the fluctuations of the local Néel order, and

$$\langle \varphi^a \rangle \propto N^a. \tag{29}$$

Now we can take the continuum limit of all the terms in the coherent state path integral for the lattice Hubbard model and obtain the following continuum Lagrangian density

$$\mathcal{L} = \overline{C}\gamma_\mu \partial_\mu C + \frac{1}{2}\left[(\partial_\mu \varphi^a)^2 + s\varphi^{a2}\right] + \frac{u}{24}\left(\varphi^{a2}\right)^2 - \lambda \varphi^a \overline{C}\rho^z \sigma^a C \tag{30}$$

This is a relativistic quantum field theory for the 8-component fermion field C and the 3-component real scalar φ^a, related to the Gross-Neveu-Yukawa model; the scalar part is the same as the

$N = 3$ case of the superfluid-insulator field theory of Lec5. We have included gradient terms and quartic in the Lagrangian for φ^a: these are not present in the derivation outlined above from the lattice Hubbard model, but are clearly induced by higher energy fermions are integrated out. The Lagrangian includes various phenomenological couplings constants (s, u, λ); as these constants are varied, $\mathcal{L}$ can describe *both* the semi-metal and insulating antiferromagnet phases, and also the quantum critical point between them.

Note that the matrix $\rho^z \sigma^a$ commutes with all the γ_μ; hence $\rho^z \sigma^a$ is a matrix in "flavor" space. So if we consider C as 2-component Dirac fermions, then these Dirac fermions carry an additional 4-component flavor index.

The semi-metal phase is the one where φ^a has vanishing vacuum expectation value (VEV). In mean-field theory, this appears for $s > 0$. The φ^a excitations are then massive, and these constitute a triplet of gapped 'spin-excitons' associated with fluctuations of the local antiferromagnetic order. The Dirac fermions are massless, and represent the Fermi point excitations of the semi-metal.

The Néel phase has a non-zero VEV, $\langle \varphi^a \rangle \neq 0$, and appears in mean-field theory for $s < 0$. Here the Dirac fermions acquire a gap, indicating that the Fermi point has vanished, and we are now in an insulating phase. The fluctuations of φ are a doublet of Goldstone modes ('spin waves') and a longitudinal massive Higgs boson.

Finally, we are ready to address the quantum critical point between these phases. In mean-field theory, this transition occurs at $s = 0$. As is customary in condensed matter physics, it is useful to carry out an RG analysis near this point. Such an analysis can be controlled in an expansion in $1/N$ (where N is the number of fermion flavors) or $(3 - d)$ (where d is the spatial dimensionality). The main conclusion of such analyses is that there is an RG fixed point at which the φ^{a2} is the only relevant perturbation. Non-linearities such as λ and u all reach stable fixed point values of order unity. This non-trivial fixed point implies that the physics of the quantum critical point is highly non-trivial and strongly coupled. The RG fixed point is scale- and relativistic-invariant, and this implies that it is also conformally invariant. Thus the quantum critical point is described by a CFT in 2+1 spacetime dimensions: a CFT3.

We will not describe the critical theory in any detail here. However, we will note some important characteristics of correlation functions at the quantum critical point. The electron Green's function has the following structure

$$\left\langle C(k,\omega); C^\dagger(k,\omega) \right\rangle \sim \frac{i\omega + k_x \tau^y + k_y \tau^x \rho^z}{(\omega^2 + k_x^2 + k_y^2)^{1-\eta_f/2}} \tag{31}$$

where $\eta_f > 0$ is the *anomalous dimension* of the fermion. This leads to a fermion spectral density which has no quasiparticle pole: thus the quantum critical point has no well-defined quasiparticle excitations. This distinguishes it from both the semi-metal and insulating antiferromagnetic phases that flank it on either side: both had excitations with infinitely-sharp quasiparticle peaks. Similar

anomalous dimensions appear in the correlations of the bosonic order parameter φ^a.

---

[1] F. F. Assaad and I. F. Herbut, "Pinning the Order: The Nature of Quantum Criticality in the Hubbard Model on Honeycomb Lattice," Phys. Rev. X **3**, 031010 (2013), arXiv:1304.6340 [cond-mat.str-el].